**KASDI MERBAHUNIVERSITY OURGLA**

**FACULTY OF MATHEMATICS AND MATERIALS SCIENCE**

**DEPARTMENT OF PHYSICS**

**MASTE'S /PROFESSIONAL THESIS IN**

**MEDICAL PHYSICS**

**ENTITLED**

# Effect of spectral slope and mean scatterer size for discrimination between different stages of hepatic fibrosis

Submitted by: **HANI sara**

**BEGGAS nour djihan**

Members of the Jury:

| | | | |
|---|---|---|---|
| **President** | BENHAMIDA Soufiane | MCA | University Ouargla |
| **Examiner** | AYAT Zahia | MCA | University Ouargla |
| **Supervisor** | REMITA Naamane | MCB | University Ouragla |

2023/2024

# Acknowledgements

*"We thank Allah for granting us the opportunity to conduct this scientific research and for blessing us with good health and well-being. We would like to express our sincere gratitude to* ***Mr. Remita Naamane*** *(Assistant Professor at the University of Ouargla) for his valuable advice and information, which greatly contributed to the completion of our study from various aspects. We also extend our thanks to all the professors in the Physics Department at the University of Ouargla. We are indebted to all of you for your support.*

*My thanks also go to* ***Mr. Pascal Laugier*** *(Director of the Parametric Imaging Laboratory, University of Paris VI) for allowing us to use the ultrasound data.*

*Finally, we would like to thank everyone who assisted us in completing this work".*

# Dedication

*I dedicate this success to my dear parents; you are the pillar on which I built all my successes.*

*To my dearest possessions, my brothers* ***"Khaled and Tarek "***

*and my sisters* ***"Warda, Abir, Chaima and Radja"***

*To my lifelong friend and constant supporter "Aicha" and to all my friends and colleagues, the partners in this long journey.*

*To the greatest team in the world* ***"Real Madrid"*** *which has given me happiness in times when I needed it.*

*And finally, thanks to myself, who was patient and diligent until I achieved*

***Sara***

# Dedication

*“To my beloved family, I want to express my deep thanks and gratitude for all the support and encouragement you have given me throughout my years of study. Without your presence and trust in me, I would not have been able to achieve this achievement. You are the pillar on which I leaned in every difficult and joyful moment. I thank you from the bottom of my heart and I dedicate this graduation goes to all my friends who shared my joy and made me happy with their support. You are part of my success and my pride, and I pray to God to bless you and protect you always with great love and gratitude to each one of you“.*

***Djihan***

# Contents

# Contents

# List of Figures

# List of Tables

# Abstract

**Abstract:**

Ultrasound imaging has been used with great success in many fields, including the medical field, especially in the study of biological tissues.

In this work, we focused on distinguishing between stages of fibrosis using mean scatterer size and spectral slope.

The results of the study showed the possibility of distinguishing between healthy and fibrotic liver tissue. However, the study did not achieve an accurate determination of the levels of fibrosis, which prompted us to test the mean scatterer sizeand the spectral slope. This achieved a positive result if we exclude the difficulty of distinguishing between the two levels (F1, F4).

**Key words:** Ultrasound, mean scatterer size, spectral slope.

**Résumé:**

L'imagerie par ultrasons a été utilisée avec un grand succès dans de nombreux domaines, y compris le domaine médical, en particulier dans l'étude des tissus biologiques.

Dans ce travail, nous nous sommes concentrés sur la distinction entre les stades de fibrose en utilisant la taille moyenne des diffuseurs et la pente spectrale.

Les résultats de l'étude ont montré la possibilité de distinguer entre les tissus hépatiques sains et fibrotiques. Cependant, l'étude n'a pas permis une détermination précise des niveaux de fibrose, ce qui nous a poussés à tester la taille moyenne des diffuseurs et la pente spectrale. Cela a donné un résultat positif si nous excluons la difficulté de distinguer entre les deux niveaux (F1, F4).

**Mots clés:** Ultrasons, la taille moyenne des diffuseurs, la pente spectrale.

**الملخص :**

تم استخدام تقنية التصوير بالموجات فوق الصوتية بنجاح كبير في العديد من المجالات، بما في ذلك المجال الطبي، خاصة في دراسة الأنسجة البيولوجية.
في هذا العمل، ركزنا على التمييز بين مراحل تليف الكبدي وذلك باستخدام متوسط حجم التشتت والانحدار الطيفي.
أظهرت نتائج الدراسة إمكانية التمييز بين أنسجة الكبد السليمة والأنسجة التي تعاني من التليف. و مع ذلك، لم تحقق الدراسة تحديدًا دقيقًا لمستويات التليف، مما دفعنا إلى اختبار متوسط حجم التشتت والانحدار الطيفي. وقد حقق هذا نتيجة إيجابية إذا استثنينا صعوبة التمييز بين المرحلتين(F1,F4).

**الكلمات المفتاحية:** الموجات فوق الصوتية ، متوسط حجم التشتت ، الانحدار الطيفي.

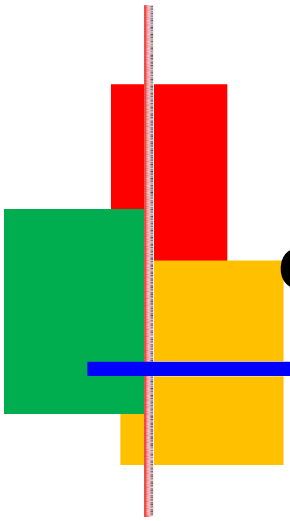

# GENERAL INTRODUCTION

# GENERAL INTRODUCTION

Ultrasound is a common technology that is used in several fields, and among these fields is its use in medical diagnosis, as it relies on sending high-frequency ultrasound waves (above 20 MHz) inside the body and measuring the response from different tissues.

Ultrasound contributes to the diagnosis of many different tumors, such as cirrhosis of the liver, which is the subject of this work.

Among the methods and techniques for diagnosing liver cirrhosis, the quantitative ultrasound characterization method is suitable because it is safe and has a low cost compared to other techniques.

Quantitative parameters are used in the analysis of radio-frequency signals (rf) to characterize liver fibrosis, and among these parameters (speed, attenuation and backscatter coefficients and mean scatterer size...).

The purpose of this research is to detect and identify the stages of hepatic fibrosis using ultrasound parameters such as mean scatterer size and spectral slope, and to evaluate the ability of each of these parameters to distinguish and separate the different stages of hepatic fibrosis.

This work was divided into four chapters:

**ChapterI:** We briefly present the anatomy and histology of the liver with its common diseases such as steatosis, fibrosis and cirrhosis, which we will focus on because it is the subject of our study and its different stages, and finally we learn about radiological methods for estimating fibrosis.

**Chapter II:** we learn about the basics of ultrasound waves to learn about their properties, and we touch on the interactions they produce on biological tissues (diffraction, attenuation, and propagation). Then we learn about ultrasound imaging and its various applications.

**Chapter III:** we describe the method for estimating the mean scatterer sizeand spectral slope.

**Chapter IV:** we presented and discussed the statistical results obtained from analyzing the ultrasound parameters mean scatterer size (MSS) and spectral slope (SSL) for different stages of fibrosis, and then concluded this study.

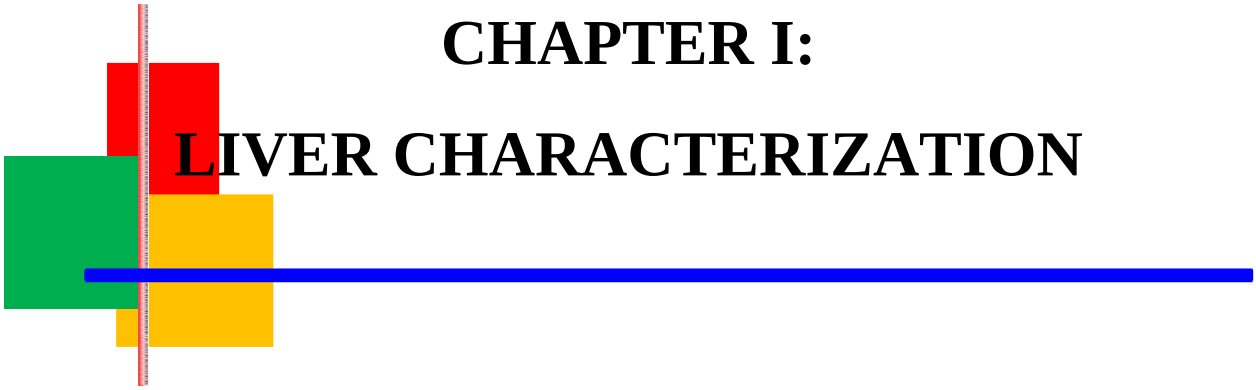

# CHAPTER I:

# LIVER CHARACTERIZATION

# CHAPTER I:LIVER CHARACTERIZATION

## 1. Introduction :

This chapter we aim to unravel the nature of the liver, considering its anatomical nuances, physiological functions, and susceptibility to various diseases.

## 2. Definition:

The liver is a football-sized organ on the right side of the abdomen, helps in food digestion and creates the substances the body needs also involved in many different processes in the body the liver is a versatile organ that contributes to metabolic activities, detoxification, and the regulation of various biochemical pathways

## 3. Liver Anatomy:

The liver is the second largest (after the skin) organ in the human body and the largest gland (weighing an average of 1500 g). It lies under the diaphragm in the right upper abdomen and mid-abdomen and extends to the left upper abdomen. The liver has the general shape of a prism or wedge, with its base to the right and its apex to the left. It is pinkish brown in color, with a soft consistency, and is highly vascular and easily friable [1]

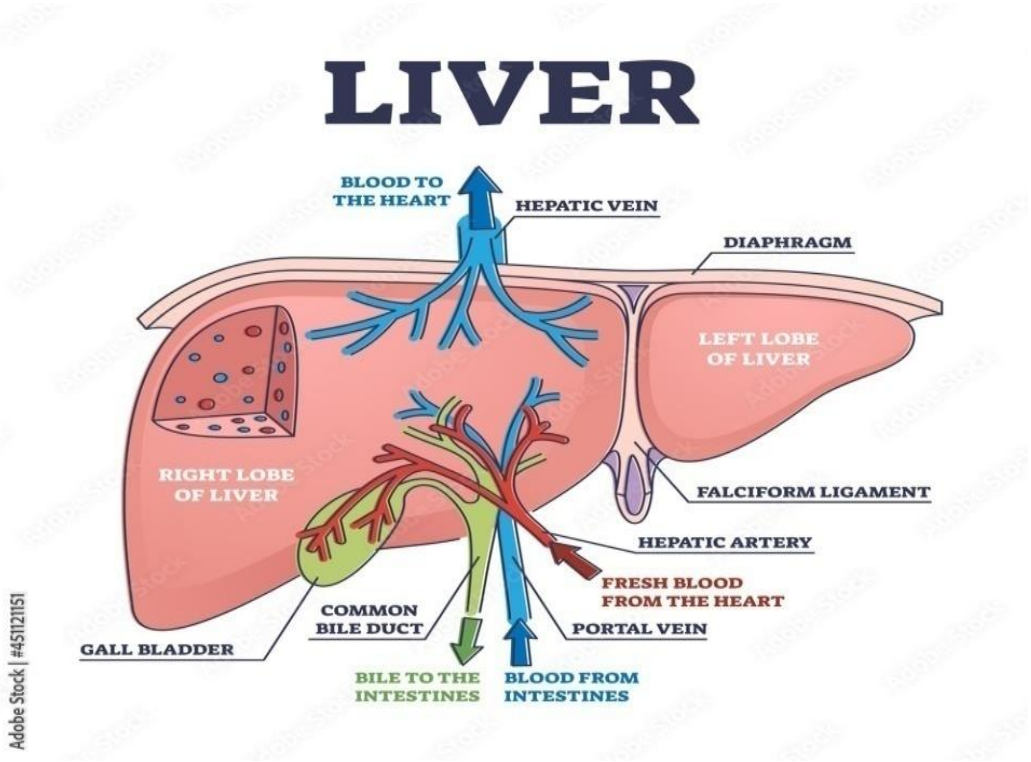


***Fig(I- 1):*** *liver anatomy illustration [2]*

### 3.1.Anatomic Divisions:

On computed tomography (CT), the portal vein branches divide the right and left lobes of the liver into superior and inferior halves. The superior half of liver is composed of (from right to left) segments VII, VIII, IVA and II; the inferior half is composed of (from right to left) segments VI, V, IVB and III.

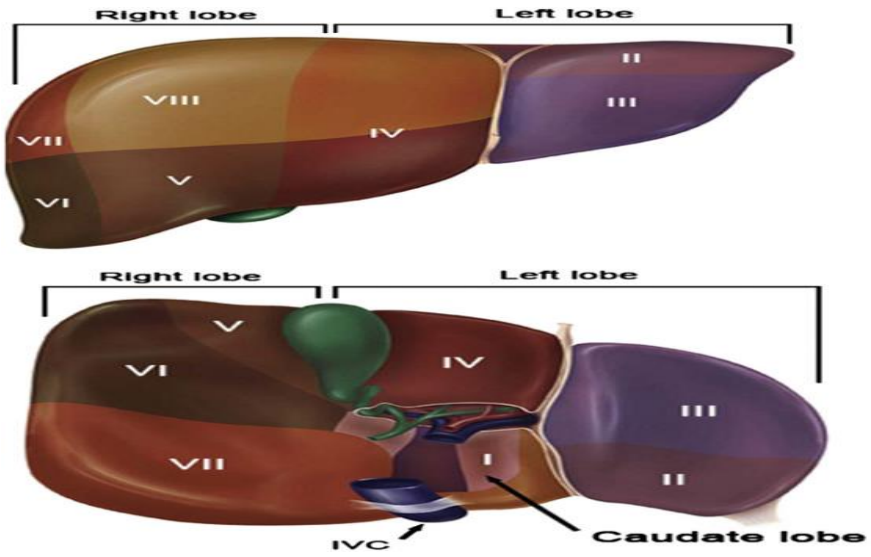


***Fig (I-2):*** *Anterior and posterior surfaces of liver illustrating functional division of the liver [3]*

### 4. Liver physiology:

The liver plays a role in nearly every organ system in the body. It interacts with the endocrine and gastrointestinal systems by aiding in digestion and metabolism. The liver is the storage location for fat-soluble vitamins and handles cholesterol homeostasis. It stores iron and copper. It plays a role in hematology with clotting factor and protein synthesis. The liver plays a role in heme breakdown into unconjugated bilirubin and conjugates it. Another critical function of the liver is metabolism and/or detoxification of xenobiotics, It plays a role in sex hormone metabolism and produces carrier proteins that are important in reproduction and development [4].

### 5. Liver diseases:

### 5.1.Steatosis liver:

Fatty liver disease (steatosis) is the build-up of excess fat in the liver cells, but if fat accounts for more than 10 per cent of the liver's weight, then it's a fatty liver.

Fatty liver may cause no damage, but sometimes the excess fat leads to inflammation of the liver. This condition, called steatohepatitis, does cause liver damage. Sometimes, inflammation from a fatty liver is linked to alcohol abuse. This is known as alcoholic steatohepatitis. Otherwise, the condition is called non-alcoholic steatohepatitis, or NASH. [5]

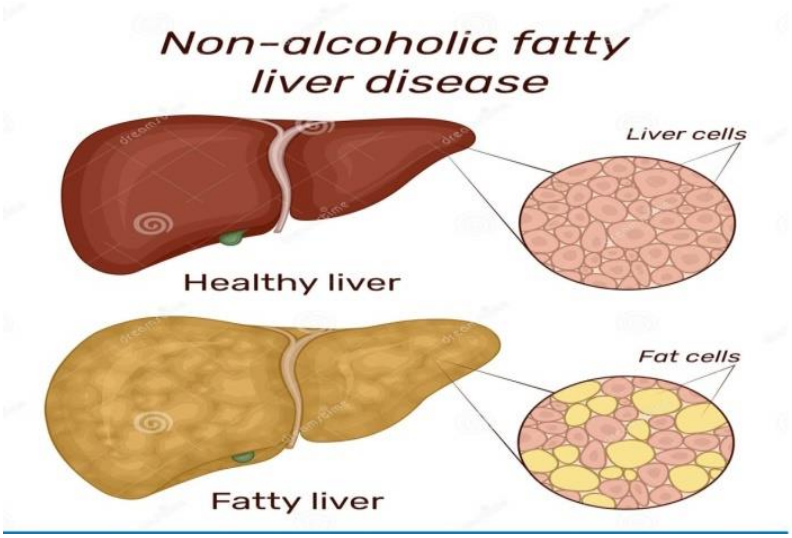


***Fig (I-3):*** *Illustration showing the difference between a healthy liver and a diseased liver [6]*

### 5.2.Liver fibrosis:

Liver fibrosis is a response generated as a result of chronic liver injury due to various factors, such as alcohol consumption, non-alcoholic steatohepatitis (NASH), viral hepatitis [hepatitis B (HBV) and hepatitis C], autoimmune hepatitis, non-alcoholic fatty liver disease (NAFLD), and cholestatic liver diseases [7]. The common effect of all of these factors on the liver is the generation of a chronic inflammation resulting in an abnormal wound healing response. Different cell types and mediators participate to encapsulate injury [8 ,9],The generation of a fibrotic response in the liver gives rise to the accumulation of extracellular matrix (ECM) components, leading to fibrous scar formation ultimately resulting liver failure[10]

#### 5.2.1. Fibroses stages:

- **Stage 1** is inflammation of your liver, caused by your immune system reacting to a foreign substance, like toxins. Chronic inflammation can lead to an enlarged liver. Inflammation can result from fatty liver, hepatitis, and other causes.

- **Stage 2** is liver fibrosis or liver scarring, caused by chronic inflammation. Scarred tissue begins to replace healthy tissue, which reduces how well your liver functions. Liver scar tissue also reduces blood flow to your liver.
- **Stage 3** is cirrhosis of your liver, caused by severe liver scarring. At the cirrhosis stage, you may experience more symptoms of liver damage including jaundice, weakness, fatigue, appetite and weight loss, abdominal bloating, and edema in your extremities.
- **Stage 4** is liver failure, which means your liver can no longer function or heal itself. In liver failure, the liver can no longer process toxins or drugs, and they build up in your body. Symptoms grow worse and can include mental and physical impairment, appetite and weight loss, diarrhea, and other problems .[11]

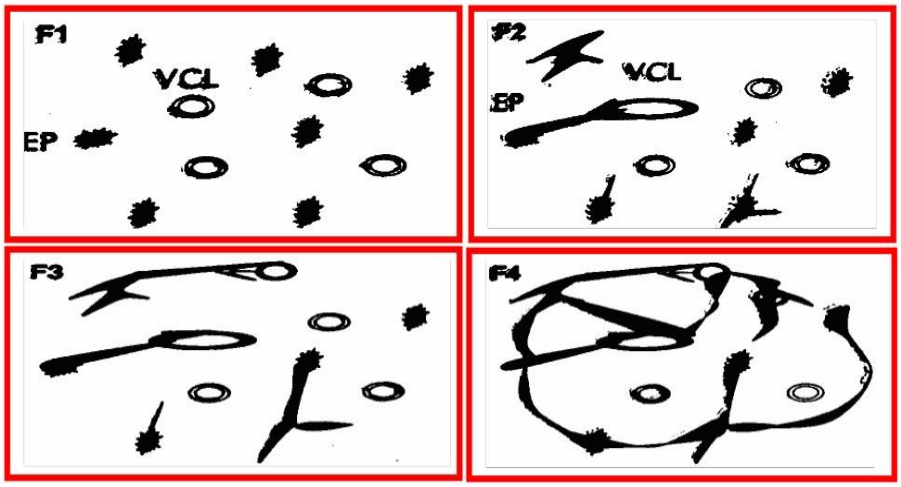


***Fig(I-4 ):****Illustration of the stages of fibrosis according to the METAVIR score (PE: portal space,VCL: centrilobularvein)[12]*

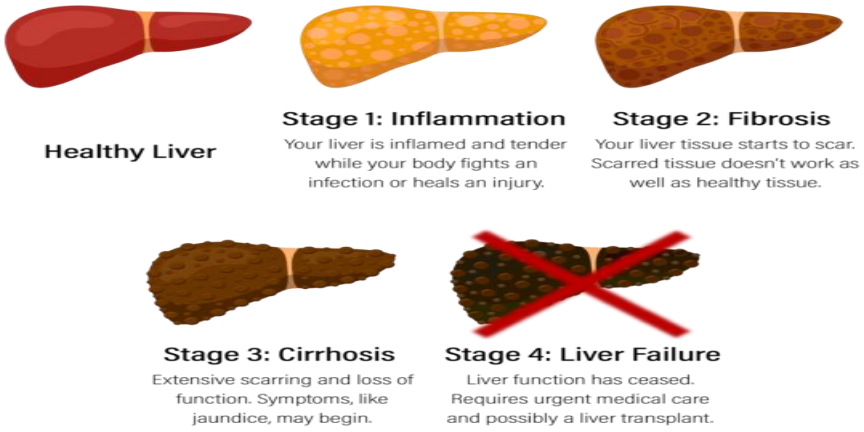


***Fig (I-5):*** *Illustration highlighting the different stages of fibrosis [13]*

### 5.3.Cirrhosis :

Cirrhosis is the ultimate stage of fibrosis, characterized by fibrosis and nodule formation of the liver, secondary to a chronic injury, which leads to alteration of the normal lobular organization of the liver. With each injury, the liver forms scar tissue (fibrosis), initially without losing its function. After a long-standing injury, most of the liver tissue gets fibrosed, leading to loss of function and the development of cirrhosis[14].

Chronic liver diseases usually progress to cirrhosis. In the developed world, the most common causes of cirrhosis are hepatitis C virus (HCV), alcoholic liver disease, and nonalcoholic steatohepatitis (NASH), while hepatitis B virus (HBV) and HCV are the most common causes in the developing world Other causes of cirrhosis include autoimmune hepatitis, primary biliary cholangitis, primary sclerosing cholangitis, hemochromatosis, Wilson disease, alpha-1 antitrypsin deficiency, Budd-Chiari syndrome, drug-induced liver cirrhosis, and chronic right-sided heart failure. Cryptogenic cirrhosis is defined as cirrhosis of unclear etiology [15].

Doctors diagnose cirrhosis based on your medical history, a physical exam, and the results of tests. Tests include blood tests, which can show signs of liver damage or infections; imaging tests; and liver biopsy [16].

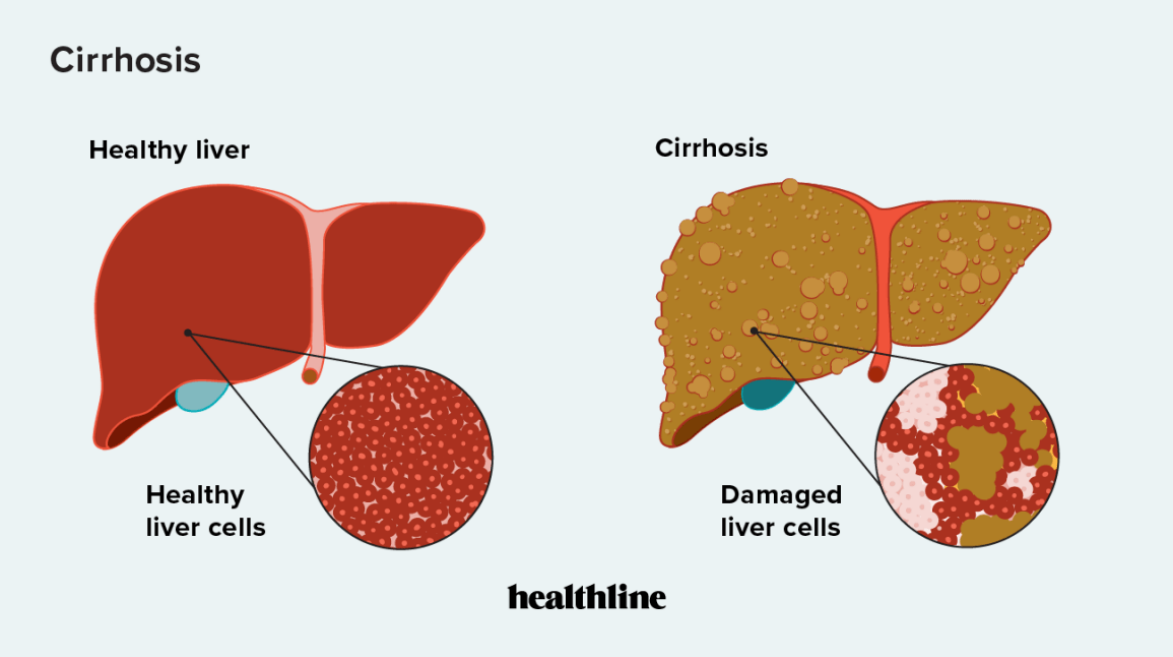


***Fig(I- 6):****Illustration showing the difference between a healthy liver and a cirrhotic liver [17]*

## 6. Liver exploration method:

### 6.1. Laboratory tests:

blood tests to check for signs of liver malfunction, such as high bilirubin levels or certain enzymes. To evaluate kidney function, blood is checked for creatinine. Serology for hepatitis virus normalized ratio (INR) is also checked for blood's ability to clot.

#### 6.1.1. Fibro test :

FibroTest-ActiTest estimates the levels of fibrosis/cirrhosis in the liver and the level of necroinflammatory activity.

6 components, 2 scores

Fibro Test combines five standard biomarkers

Gamma-GT, Total bilirubin, Alpha-2-macroglobulin , Apolipoprotein , A1 HaptoglobinActiTest adds a direct marker for inflammatory activity: Alanine aminotransferase (ALT)

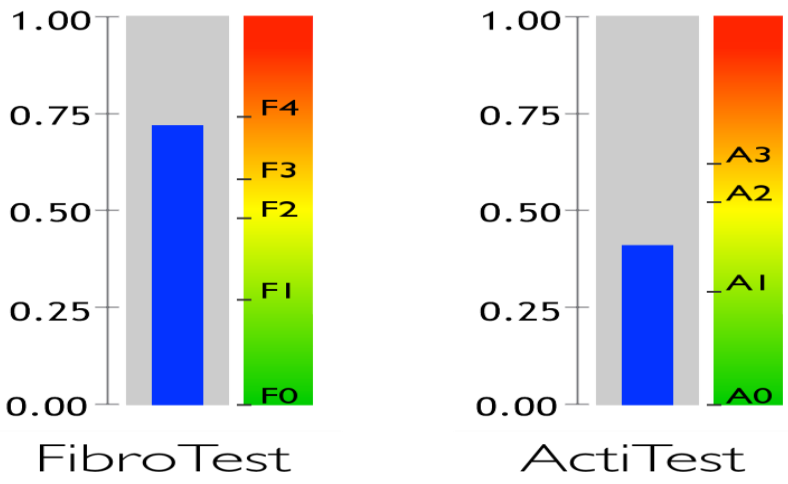


***Fig(I -7):****conversion between FibroTest and fibrosis stage*
*conversion between ActiTest and activity grade[18]*

### 6.2.Biopsy:

Liver biopsy stands as the gold standard for diagnosing and assessing liver fibrosis, offering crucial information on both the grade and the stage the use of liver biopsy is not without limitations, given its invasiveness and associated risks. In ideal circumstances, it may inaccurately stage fibrosis about 20% of the time due to sampling error and interobserver variability. Consequently, the increasing use of noninvasive methods for assessing fibrosis is

becoming prevalent, potentially replacing liver biopsy for determining fibrosis severity in individuals

### 6.2.1. Metavir Score:

The METAVIR scoring system is a method used to assess the extent of inflammation and fibrosis through histopathological evaluation in a liver biopsy of patients with hepatitis C. The Metavir scoring system rates the progression of fibrosis on a scale from A0 to A3:

- A0: no activity
- A1: mild activity
- A2: moderate activity
- A3: severe activity

The Metavir system also scores the level of fibrosis from F0 to F3:

- F0: an absence of fibrosis
- F1: portal fibrosis with no septa
- F2: portal fibrosis with infrequent septa
- F3: numerous septa but no cirrhosis
- F4: cirrhosis

The most advanced type of fibrosis someone can have before developing cirrhosis, according to the Metavir system, is stage A3F3. [19]

***Table (I-1):*** *Metavir scoring system [20]*

| **Activity score (A)** | **Fibrosis score (F)** |
|---|---|
| A0=no activity | F0 =no fibrosis |
| A1=mildactivity | F1=portal fibrosis without septa |
| A2=moderateactivity | F2= portal fibrosis with few septa |
| A3=severeactivity | F3=numerous septa without cirrhosis |
| | F4=cirrhosis |

### 6.3.Radiologic modalties to estimate fibrosis:

Imaging tests can show the size, shape, and texture of the liver and show how much fat is in the liver. Some tests can also measure the stiffness of the liver. Cirrhosis increases liver stiffness

#### 6.3.1. Ultrasound :

While hepatic ultrasound offers a noninvasive and cost-effective means of evaluating various aspects of liver health, it is important to acknowledge its limitations. Standard ultrasound, although useful in detecting certain features like liver surface nodularity and assessing blood flow, has demonstrated low sensitivity in identifying cirrhosis, hovering around 40%. False-positive readings by radiologists can pose a challenge, particularly when more definitive signs of portal hypertension are absent. [21]

#### 6.3.2. Magnetic Resonance Elastography:

Magnetic resonance elastography involves applying a probe to a person's back, emitting low-frequency vibrations through the liver, which then are measured through magnetic resonance imaging spin echo sequence. A meta-analysis of five trials comparing magnetic resonance elastography to liver biopsies showed a sensitivity of 94% and specificity of 95% in differentiating F0 to F1 from F2 to F4, as well as a sensitivity of 98% and specificity of 94% in differentiating F0 to F3 from F4. This technique shares the same limitations as transient elastography. The utility of this method in comparison to other modalities is yet to be fully elucidated. [22]

#### 6.3.3. Transient Elastography:

Transient elastography, specifically using Fibro-Scan, has emerged as a valuable noninvasive tool for assessing liver fibrosis. This diagnostic test, which typically takes only 5 to 10 minutes to complete, is convenient and can be performed in a clinic or office-based setting. One of its advantages over liver biopsy is that it examines a larger area of liver tissue, approximately 1 cm in diameter by 5 cm in length. This broader assessment may offer a more representative evaluation of the entire hepatic parenchyma.

The procedure involves the use of an ultrasound transducer probe to measure shear wave velocity, directly correlating with liver stiffness. The United States FDA approved transient elastography, specifically Fibro-Scan, in 2013, indicating its reliability and safety [23]

However, when interpreting the results of transient elastography, it's crucial to consider cutoff values. In 2005, studies by Castera and Ziol provided optimal transient elastography cutoff values that correlated with different Metavir fibrosis scores. Despite both studies utilizing the same type of transient elastography machine (FibroScan/EchoSens), they reported distinct cutoff values. These variations may be attributed to differences in study design and patient populations.

Notably, for Metavir F3 fibrosis, the cutoff values derived from both studies were nearly identical. This consistency adds reliability to the utility of transient elastography in diagnosing liver fibrosis, especially in the advanced stages. Nonetheless, clinicians should be aware of the potential variability in cutoff values and consider the specific context of each patient when interpreting results.

### 6.3.4. Shear Wave Elastograph:

Shear wave elastography is a noninvasive sonographic test that can estimate hepatic fibrosis. The test is performed by watching a real-time image with B-mode ultrasound, and then measuring liver stiffness based on anatomical information; the test also can assess liver homogeneity based on the color images it generates that correlates with varying degrees of liver stiffness. Based on limited data, shear wave elastography performs with similar accuracy as transient elastography in estimating hepatic fibrosis [24, 25].

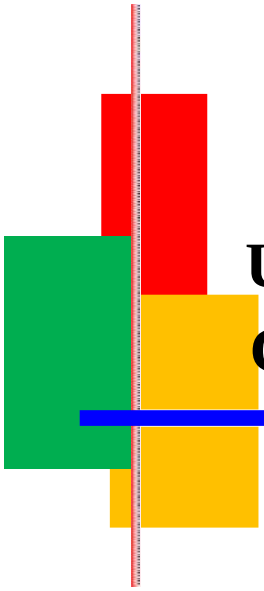

# CHAPTER II:

# ULTRASOUND WAVES CHARACTERIZATION

# CHAPTER II:ULTRASOUND WAVES CHARACTERIZATION

## 1. Introduction:

In this chapter, we will learn about the basics of ultrasound waves and their nature, and we will discuss phenomena of interaction and acoustic parameters that occur between tissues and ultrasound waves. Finally, we will explore the applications of ultrasound waves.

## 2. History of the ultrasound:

The first real breakthrough was in 1880, when **Pierre Curie** discovered the piezoelectric effect in certain crystals. **Paul Langevin** applied this in the early twentieth century as the basis for a transducer containing a piezoelectric crystal, capable of both generating an ultrasonic beam and receiving the returning echoes from interfaces between surfaces of substances of two differing acoustic impedances. This is still fundamental to the ultrasound transducers in use today.[40]

A number of pioneers, including scientists, engineers and clinicians, have contributed to the development of diagnostic ultrasonography, during the early 1940s, the Austrian neurologist **Karl Theodore Dussik** was probably the first physician to use ultra sound for diagnostic purposes. Although **John Wild** published a landmark study of breast nodules reporting a diagnostic accuracy of 90%, the Glasgow obstetrician **Lan Donald** was responsible for the ultrasound boom in medical diagnosis. In 1956, in partnership with a young engineer, **Tom Brown**, **Donald** developed the first two-dimensional, direct contact scanner in 1956, which he first demonstrated at a clinical meeting of obstetricians at the University Department of Midwifery in Glasgow [26]. Many physicians in the audience were totally opposed to the idea of relying on a machine instead of their hands when examining an unborn baby until, there and then, a Glasgow professor of Internal Medicine happened to make a diagnosis of malignant ascites in a female patient. On examining the patient himself with the ultrasound machine, Professor **Donald** informed the audience that the finding looked more like an ovarian cyst. Definite clinical interest was aroused when this diagnosis was confirmed in operating theatre [26].

## 3. Ultrasound definition:

An ultrasound is a type of oscillating sound pressure wave that has a higher frequency than human hearing is able to detect. An ultrasound is not a unique type of sound, therefore, but is classified differently due to the fact that humans cannot hear it. Ultrasounds have a

frequency greater than 20 kHz, which is beyond the frequency limit of sounds that humans are able to hear [27].

Ultrasonic diagnosis has been widely used in the clinical medicine. However, contemporary ultrasonic diagnosis technique is limited to the qualitative description at frequency ranging between 0.5-10 MHz based on the gray scale presentation in ultrasonic image. Due to the longer wavelength at a low frequency, the image resolution is not very high. Besides, the physical quantity using the ultrasonic image is the amplitude of the echo while the spectrum of the echo is overlooked [28].

### 3.1.The nature of ultrasound:

Ultrasonic waves are waves of frequency above the audible frequencies the human ear. In medical diagnostics are used ultrasound frequencies between 3 and 10 MHz. The most important parameters describing the wave are [29]:

• Wavelength

• Frequency

• Velocity

• Intensity

### 3.2. Generating ultrasound waves:

Ultrasound waves are generated by a transducer consisting of a disc with crystals of lead zirconate titanate. These crystals are piezoelectric, in other words they transform electrical potentials into mechanical vibrations and vice versa. Every time an electrical current is passed through the crystals, the disc generates an ultrasound pulse; conversely, when the disc receives a wave of ultrasound, it will deform and a voltage is generated on the transducer surface. To produce a well-directed beam, the disc is mounted at the end of a cylindrical tube, also called a probe. At the other end of the tube, damping material is mounted to damp down the ultrasonic waves generated at the back of the disc [26].

### 4. Ultrasonic transducers:

Medical ultrasound transducer (echo-scopic probe) is a device that is placed on the patient's body and contains one or more ultrasonic transducers. We can distinguish: [29]

• Linear probe

• Sectoral probe

• Probe, in which the ring changer focusing is performed

• Rocking mirror test

• Convex probe

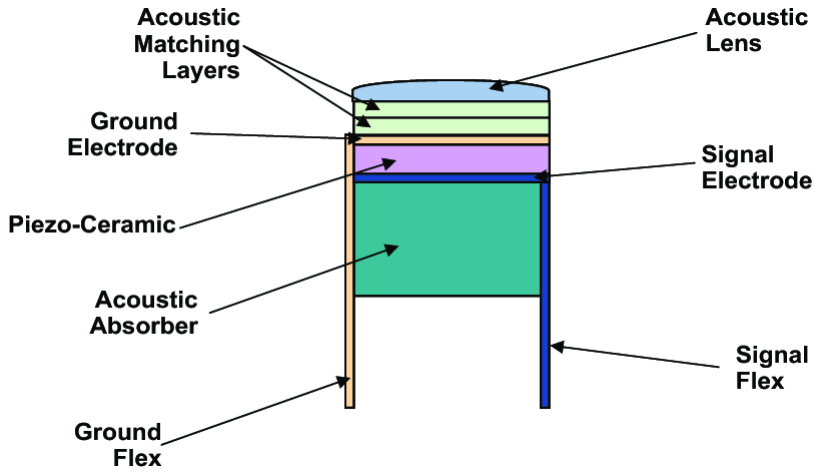


*Fig (II-1):Ultrasound Transducer Cross-Sectional View[36]*

### 5. Acoustic parameters:

### 5.1. Attenuation:

Ultrasound loses its energy as it propagates through a tissue. This loss of energy is called attenuation. There are three causes of attenuation: diffraction, scattering, and absorption. Attenuation results in echoes from deep body tissues being displayed less intensely then those returning from superficial structures.[26]

The acoustic intensity$I(z)$decreases exponentially with the depth z of ultrasound penetration into the medium. It is expressed by the relationship [ 32]:

$$I(z) = I_0 e^{-\alpha.z}$$

Where α designates the attenuation coefficient.

### 5.2. The acoustic impedance:

The velocity of sound within each tissue and the tissue's physical density determines the percentage of the beam reflected or transmitted as it passes from one tissue boundary to another or to different boundaries within a given tissue. The product of the density by the propagation speed in the medium considered is known as the tissue's acoustic impedance "z"[32]. It is defined by[30]:

$$z\,(kg/m^2 s) = \rho c = \sqrt{\frac{\rho}{K}}$$

ρ : the density of fluid

c: speed of the wave

k: the compressibility

It is the difference in acoustic impedance between the tissues that accounts for the reflectivity of a given tissue. The amplitude of the returned echo is proportional to the difference in acoustic impedance between two tissues as the sound beam passes through their interface. There are only small differences in the acoustic impedance among the body's soft tissues.[34]

***Table (II-1)**: shows the average values of acoustic impendence of various tissues* [31]

| **Body tissue** | **Acoustic impedance (106 Rayls)** |
|---|---|
| Air | 0.0004 |
| Lung | 0.18 |
| Fat | 1.34 |

| | |
|---|---|
| Liver | 1.65 |
| Blood | 1.65 |
| Kidney | 1.63 |
| Muscle | 1.71 |
| Bone | 7.8 |

### 5.3. Velocity of ultrasound:

The ultrasound wave is characterized by its frequency f (Hz) and its wavelength λ(m). These two characteristics make it possible to determine the velocity of propagation of ultrasound in the environment [30].

$$c(m/s) = \sqrt{\frac{1}{K\rho}}$$

Where K represents compressibility andρ the density.

Frequency and wavelength are inversely related if the sound velocity within the medium remains constant. Because sound velocity is independent of frequency and nearly constant (1540 m/sec) in the body's soft tissues, selecting a higher frequency transducer will result in decreased wavelength of the emitted sound, providing better axial resolution. The relationship between velocity, frequency, and wavelength can be summarized in the following equation.[34]

Velocity (m/sec) = frequency (cycles/sec) × wavelength (m/cycle)

***Table (II-2)**: velocity of ultrasound in tissue*[33]

| **Medium** | **velocity of ultrasound (ms-1)** |
|---|---|
| Air | 331 |
| Muscle | 1585 |
| Fat | 1450 |
| Soft tissue (average) | 1540 |

### 6. Interaction phenomena:

As the ultrasound wave travels through tissues, it is subject to a number of interactions. The most important features are as follow [37]:

- Reflection
- Scatter
- Absorption

#### 6.1. Reflection:

The waves emitted are reflected at the interface of two different tissues. The greater the difference in tissue density, the more reflective the boundary will be, while with similar densities waves pass easily through the tissues.[26]

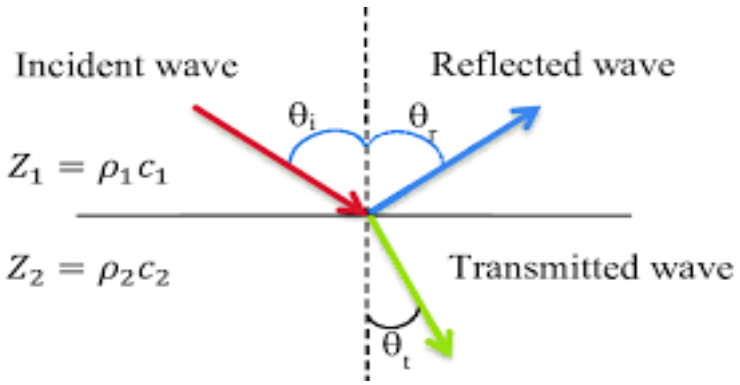


***Fig(II-2)**:Transmission and reflection of an ultrasound wave between two different media with different acoustic impedance $Z_1$and $Z_2$. An incident angle $\theta_i$lead to reflected angle $\theta_r$=$\theta_i$ and a transmitted angle $\theta_t$*[35].

The intensity reflection coefficient R and transmission coefficient T are given by[35]:

$$R = \frac{I_r}{I_i} = \frac{(Z_1 \cos\theta_t - Z_2 \cos\theta_i)^2}{(Z_1 \cos\theta_t + Z_2 \cos\theta_i)^2}$$

and

$$T = \frac{I_t}{I_i} = \frac{4Z_1 Z_2 \cos\theta_i \cos\theta_t}{(Z_1 \cos\theta_t + Z_2 \cos\theta_i)^2}$$

Where $I_i$ , $I_r$ and $I_t$ are the intensities of the reflected and transmitted incident waves respectively and $z_1$,$z_2$are the acoustic impedances corresponding to environments 1 and 2 respectively [32].

If the incident wave arrives perpendicularity to the interface of the two media (Ti= 0°), the transmitted angle is also equal to 0° and the coefficient Rand Tare[35]:

$$R = \frac{I_r}{I_i} = \frac{(z_2 - z_1)^2}{(z_2 + z_1)^2}$$

and

$$T = \frac{I_t}{I_i} = \frac{4z_1z_2}{(z_2 + z_1)^2}$$

***Table (II-3)****: shows the percentages of reflection coefficient in different interfaces*[35]

| Interface | Reflection coefficient (%) |
|---|---|
| Soft tissue - Air | 99 |
| Soft tissue - Bone | 66 |
| Fat - Muscle | 1.08 |
| Muscle - Liver | 1.5 |

### 6.2.Scattering of ultrasound:

When the reflecting interface is irregular in shape, and its dimensions are smaller than the diameter of the ultrasound beam, the incident beam is reflected in many different directions. This is known as non-specular reflection, or scattering. The direction of scatter does not obey the simple law of reflection as in specular reflection, but depends instead on the relative sizes of the scattering target and the ultrasound beam diameter. Therefore, energy incident upon the small target at quite large angles of incidence will have a chance of being detected at the transducer. The dimensions of the interface should be about one wavelength of the ultrasound beam or less for scattering to occur[39].

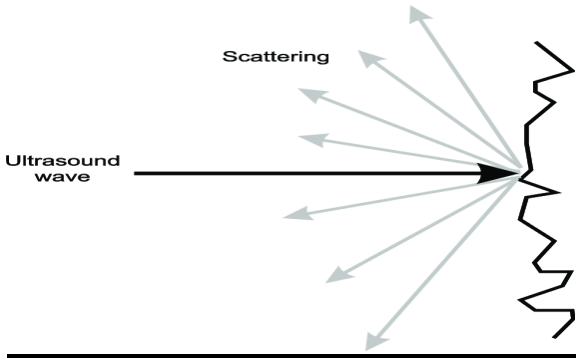


***Fig (II-3)**: Scattering of ultrasound wave*[ 38]

### 6.3. Absorption:

Absorption is defined as the direct conversion of the sound energy into heat. In other words, ultrasound scanning generates heat in the tissue. Higher frequencies are absorbed in a greater rate than lower frequencies. However, a higher scanning frequency gives a better axial resolution. If the ultrasound penetration is not sufficient to visualize the structures of interest, a lower frequency is selected to increase the penetration. The use of longer wavelengths (lower frequency) results in lower resolution because the resolution of ultrasound imaging is proportional to the wavelength of the imaging wave.[37]

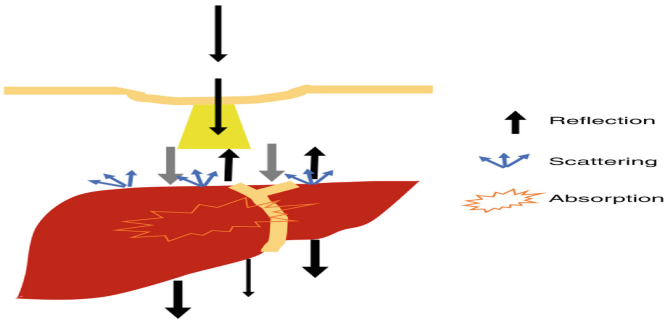


***Fig(II-4)**:Absorption of ultrasound* [31]

## 7. The ultrasound image:

An ultrasound image is generated when the pulse wave emitted from the transducer is transmitted into the body, reflected off the tissue interface, and returned to the transducer.

The image can be displayed in a number of modes:

- Amplitude (A) mode is the display of amplitude spikes in the vertical axis and the time required for the return of the echo in the horizontal axis.
- Brightness (B) display a tow-dimensional map of the data acquired and is most commonly used for ultrasound guided intervention.
- Motion (M) mode, also called time motion or TM mode, displays a one-dimensional image usually used for analyzing moving body parts. This mode records the amplitude and rate of motion in real time and is commonly used in cardiovascular imaging.[31]

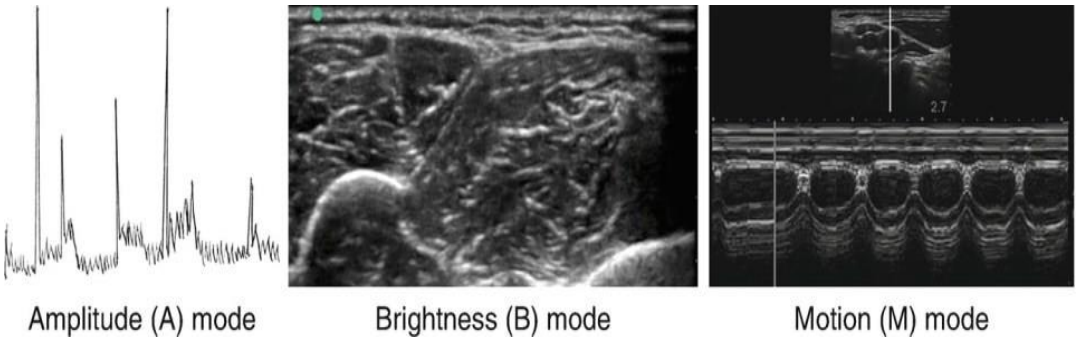


***Fig (II-5)**: Three different modes of ultrasound* [31]

The principle of ultrasound imaging is as follows: an electrically excited transducer emits a short duration ultrasonic signal, commonly referred to as a "pulse," into a biological medium. The reflected or scattered echoes return to the ultrasound transducer with a delay that depends on the distance to the reflecting (or scattering) structure. This transducer converts the received acoustic signal into an electrical signal called "radiofrequency ultrasound signal" (rf). In the presence of a large number of scatterers, the ensemble of scattered wavelets can interfere at the transducer surface. The rf signal is rectified and then detected (video signal) or enveloped and converted into grayscale levels which are displayed in the image.[32]

The ultrasound image is reconstructed from the ultrasound signals collected by the transducer and transmitted to the device. The information is processed by complex software that allows determining the position and intensity of the echo and representing the signal (or image) to be interpreted by the operator. By replicating the same process for different positions along the same direction (perpendicular to the beam axis), we then obtain an image in a plane.[32]

## 8. Some applications of ultrasound :

• It is used in security systems to detect even the slightest movement in a specified area.

• Ultrasound is used in industry to analyze the uniformity and purity of liquids and solids by means of acoustic microscopy.

• It is used in humidifiers in which ultrasound waves vibrate a metal sheet to spray the water as a fine mist.

• Ultrasonic welding is used to create heat to weld plastics.

• Ultrasonic cleaning is useful to clean delicate articles of jewelry, watches and lenses.[41]

## 9. Conclusion:

In this chapter, we focused on the ultrasound waves and their propagation in biological tissues, discussed the role of ultrasound transducer device, as well as mentioned acoustic phenomena and parameters, and explored the applications of ultrasound waves.

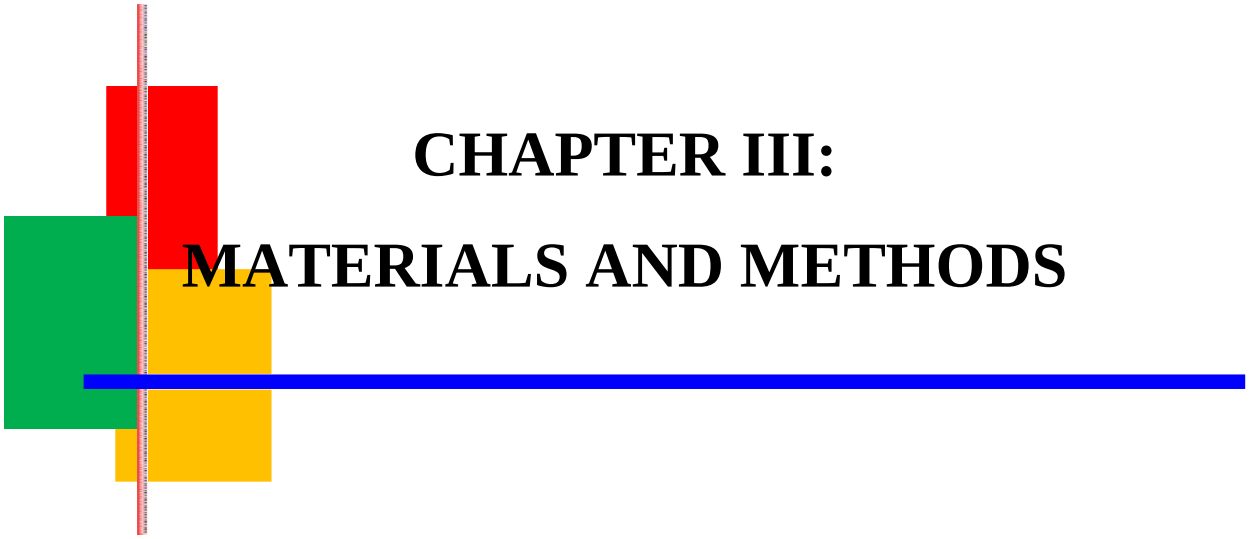

# CHAPTER III:

# MATERIALS AND METHODS

# CHAPTER III: MATERIALS AND METHODS

**Introduction:**

In this chapter, we present a method for estimating the mean scatterer size from backscattering curves. Before introducing this method, we firstly present a model of radiofrequency (RF) signal, which forms the basis of quantitative imaging. A model of ultrasound signal is proposed (Chapter I). This simple model helps in better understanding the various phenomena (diffraction, attenuation, and scattering (backscattering)) occurring on the ultrasonic wave during its propagation from the transducer to the medium and vice versa.

## 1. Methods for estimating acoustic parameters from RF signals:

### 1.1.Experimental device:

Central to this setup is a tank housing the liver sample, submerged in a solution of physiological serum at a controlled temperature of 35±2°C. The ultrasound component comprises a 20MHz transducer and a pulse generator with a bandwidth of 200MHz (Sofranel 5900 PR), which operates in transmission/reception mode. This generator emits short-duration electrical pulses that excite the transducer, facilitating the transmission of ultrasound waves through the sample.

The signal backscattered by the sample is captured by the transducer and sampled by a high-speed digital oscilloscope (Lecroy Co, New York, USA, model 9450A) at a rate of 100MHz, with 8-bit resolution. These signals are then stored in the memory of a PC along with acquisition conditions for subsequent analysis. The PC runs the US 2000 acquisition software, which not only manages motor displacement commands but also records ultrasound signals, ensuring seamless operation and data management.

The motor assembly, situated on a vibration-resistant table from Micro control (France), facilitates precise movement of the ultrasound probe in three dimensions: 0.1 μm for horizontal movement (XY) and 1 μm for vertical movement (Z). Additionally, a fourth motor enables controlled rotation of the transducer axis in a vertical plane, with an impressive precision of 0.01°.

Sample scanning is conducted systematically, with a step size of 200 μm in both horizontal directions (XY),

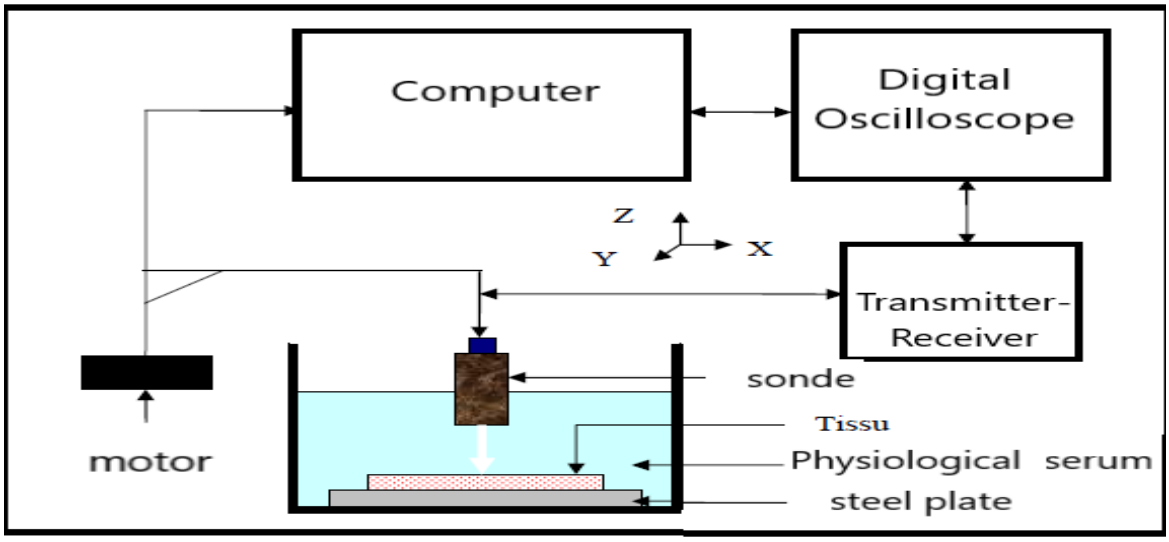


***Fig (III.1):*** *Schematic representation of the experimental device used for ultrasonic acquisitions performed at 20 MHz .*

**1 .2. Ultrasound Transducer Features:**

In this work, the exploration of human liver samples was carried out with a probe of PANAMETRICS M316 type with central frequency $f_c = 20\ MHz$ which has the following characteristics: (an active diameter a and a focal length F which have respective values of 3.1 mm and 20 mm). At -6 dB the probe has a bandwidth of (6-30) MHz and lateral resolutions of 460 µm and axial resolution of 75 µm (with a speed of 1540 m/s).

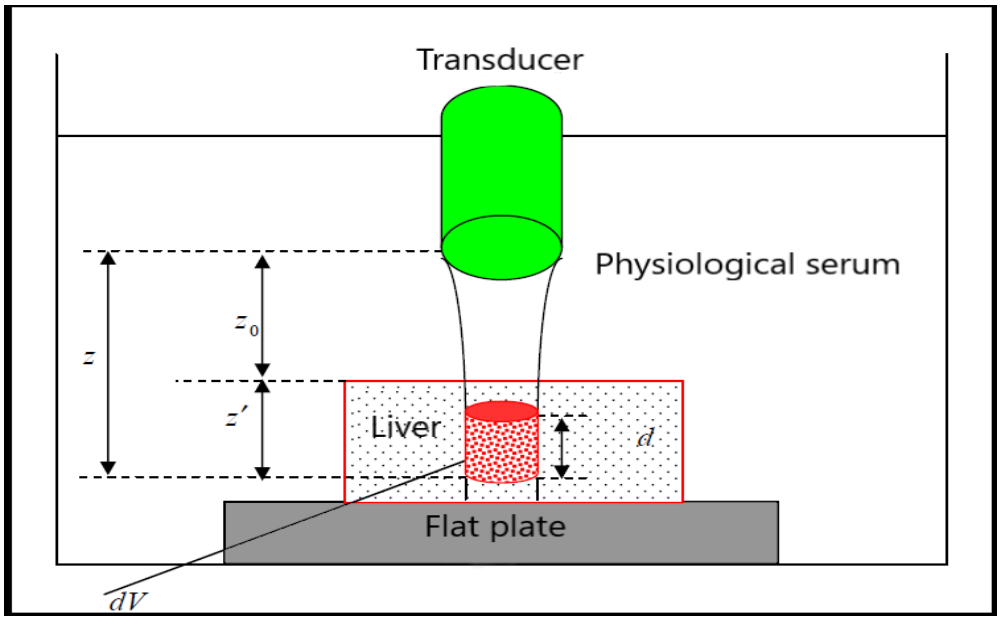


***Fig (III.2):*** *Representative diagram of the volume insonified by a focused transducer with the notations used in the equations*

The signal backscattered by a volume dV, *(*Fig.III.2), located at distance z from the internal matrix of the tissue can be described, in the frequency domain, according to equation (IIII-1) as follows:

$$S(M_i, f) = E(f)H(f)D^2(M_i, f)A^2(M_i, f)R(M_i, f) \quad \textbf{(III-1)}$$

Where:

*E* (*f*): the Fourier transform of *e* (*t*)

*H* (f) *t:* the Fourier transform of *h* (*t*)

*D* ($M_i$, *f*): the Fourier transform of *d* ($Mi_i$, *t*)

*A* ($M_i$, *f*): the Fourier transform of a ($M_i$, *t*)

*R* ($M_i$, *f*): the Fourier transform of *r* ($M_i$, *t*)

$$S(z, f) = E(f) \times H_t(f) \times A^2(z, f) \times D^2(z, f) \times T_f^2 \times R(z, f) \quad \textbf{(III-2)}$$

Where $T_f^2$ is the coefficient of double transmission at the water/liver interface.

This relationship assumes that the axial and lateral dimensions of the volume $(dV)$ are small compared to the dimensions$(z)$. Thus, the attenuation term can be considered constant for all points within this volume, and therefore we can assume that the term $A^2(Mi, f)$ becomes $A^2(z, f)$. Where $(z)$ is the distance separating the beginning of the measurement volume $(dV)$ from the transducer, $E(f)$ is the signal emitted by the pulse generator, $H_{t(f)}$ is the transfer function including electro-acoustic, acousto-electric conversions, and the device function. $A^2(z, f)$ is the attenuation transfer function in physiological serum thenin the tissue above the explored volume $(dV)$, $D^2(z, f)$ is the diffraction term for all scatterers within an isochronous volume. $R(z, f)$ represents the coefficient of backscattering induced by the presence of scatterers within the volume. We can express the attenuation term $A(z, f)$ to separate the attenuation effects at the level of physiological serum from the sample as follows:

$$A(z, f) = A_0(z_0, f) \times A_{liver}(z', f) \textbf{(III-3)}$$

Where:

$A_0(z_0, f)$ represents attenuation at the level of physiological serum.

$A(z', f)_{liver}$ represents attenuation at the level of the liver.

$z_0$ : The distance between the probe and the anterior face of the sample.

$$z_{liver} = z - z_0$$

The estimation of quantitative ultrasound parameters, in ultrasound mode, is based on the assumption of a medium in which scatterers are distributed randomly and uniformly (in this case, it is referred to as a statistically homogeneous medium). In other words, this means that in the measurement zone, the backscattering transfer function does not depend on the position $(M)$ of the scatterers, but only on the frequency $(f)$, thus $R(M,f)$ becomes $R(f)$[42]. Under these conditions, equation (III-2)) can be written as:

$$S(z,f) = G(f) \times A_0^2(z_0\ ,f) \times A_{liver}^2(z',f) \times D^2(z\ ,f) \times T_f^2 \times R(f) \textbf{(III-4)}$$

$T_f^2$: Transmission coefficient

$G(f) = E(f) \times H_t(f)$ (a term dependent on the source).

$D^2(z,f) and\ A^2\ (z,f)$ depend on the position, and $R(f)$ depends on the scatterer.

The assumptions allowing for the modeling of equations (III-2) and (III-4) are as follows:

- The distances $(z)$ between all points of the transducer and the scattering volume $(dV)$ are assumed to be equal and sufficiently large compared to the dimensions of the transducer, so that the effects of attenuation and diffraction are completely separated.
- The dimensions of the volume $(dV)(dx,dy,dz)$ are small enough compared to the distance z. Thus, the attenuation term can be assumed constant for all points of$(dV)$. Using this approximation, the term $D_v^{2\ \square}(z\ ,f)$ can be calculated by integrating the diffraction function over the volume$(dV)$.
- The explored surface of the liver must be relatively flat.

## 2. Estimation of Quantitative Parameters:

### 2.1.Backscattering Coefficient:

For the backscattering coefficient, we will limit ourselves to recalling the essential steps to facilitate the understanding of its relationship with the structure of hepatic tissue. For more details, reference can be made to various studies conducted by Insana [43], Roberjot[44], Wear [45].

#### 2.1.1. The evaluation of the backscattering coefficient:

The evaluation of the backscattering coefficient is not an easy task in itself because it must be independent of the measurement system. Therefore, it is necessary to eliminate the effects

of the ultrasonic acquisition chain, starting with diffraction effects related to the probe geometry and attenuation effects during wave propagation in the liver [46]. To achieve this, we acquired ultrasound signals on a perfectly flat steel plate immersed in physiological saline solution (reference signal). Using micrometric motors, we varied the distance (z) between the transducer and the plate. At each position, an ultrasound signal was acquired. The transducer was moved in steps of 500 µm along the direction of wave propagation (z-axis) to record ultrasound signals at the focal point and on either side of it. For each ultrasound signal, the corresponding power spectrum was evaluated. In the end, we obtained a series of power spectra which constitute what we called the reference spectrum, which can be modeled by the relationship.

$$S_{ref}(z,f) = G(f) \times A_0^2(z_0,f\ ) \times D_s^2(z,f) \times R_{p(f)} \textbf{(III-5)}$$

Where $Rp$ represents the reflection coefficient of the planar reflector and $D_s$ represents the diffraction function in physiological saline solution.

The distance z covered by the transducer must at least span the region where the sample is located. Figure III.3 illustrates the different ultrasound lines obtained at various distances z from the plate.

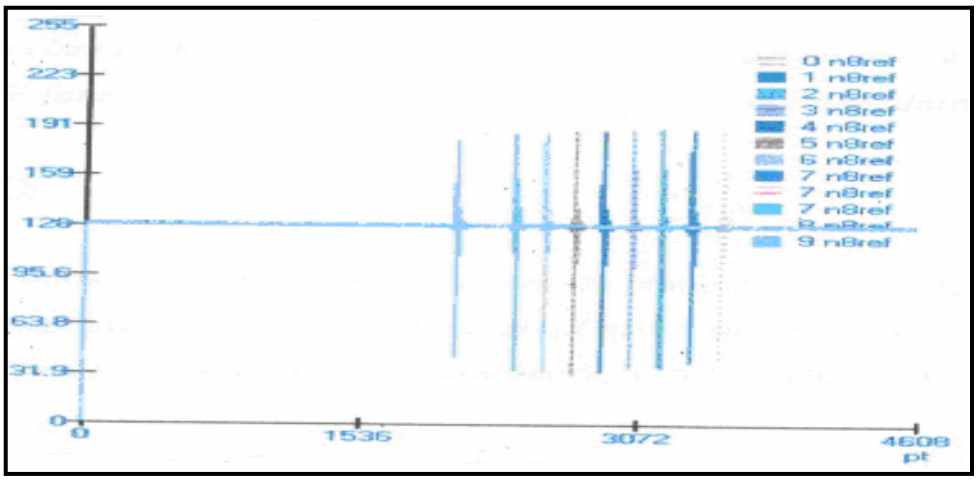


***Fig (III.3):*** *Illustration of the ultrasound lines used in correcting the diffraction effect of the ultrasound beam.*

The programs we used for the evaluation of certain parameters rely on the segmentation of radiofrequency signals (short-time Fourier analysis). It is therefore necessary to determine the duration of these segments (windows). It should also be noted that for the backscattering coefficient, the RF signals require what is called realignment.

The estimation of the corrected mean backscattering curve accounting for attenuation effects, denoted as $\mu(z,f)$ and expressed in dB, is obtained following the work of Roberjot et al [44], and is expressed as follows:

$$\mu(z,f)_{dB} = 10\log_{10}\left[\frac{\langle|S(z,f)|^2\rangle}{|S_{ref}(z,f)|^2}A(z,f).\frac{1}{(0.63)^2}.\frac{1}{d}\frac{R_p^2K^2a^2}{8\pi\left[1+\left(\frac{ka^2}{4F}\right)^2\right]}\right] \quad \text{(III–6)}$$

Where: $f$ is the frequency.

$\langle|S(z,f)|^2\rangle$ =Mean spectrum of the signal backscattered by a volume dV of the sample located around depth z and delimited by the width of the beam at this depth and by the size of the segmentation window.

$|S_{ref}(z,f)|$ =Spectrum of the signal reflected by a flat reflector placed at the focal distance of the transducer.

$A(z,f)$Representing the attenuation correction term.

The last term of equation (III-6) compensates for the frequency dependence effects of the ultrasonic beam profile, where "$a$" represents the radius of the transducer, "$k$" is the wave number, "$R_P$" is the amplitude reflection coefficient on the flat plate (assumed to be one for a perfect reflector), "$d$" is the thickness of the segmentation window, and "$F$" is the focal distance of the transducer.

$\frac{1}{(0.63)^2}$ Represents the compensation for the Hamming window function.

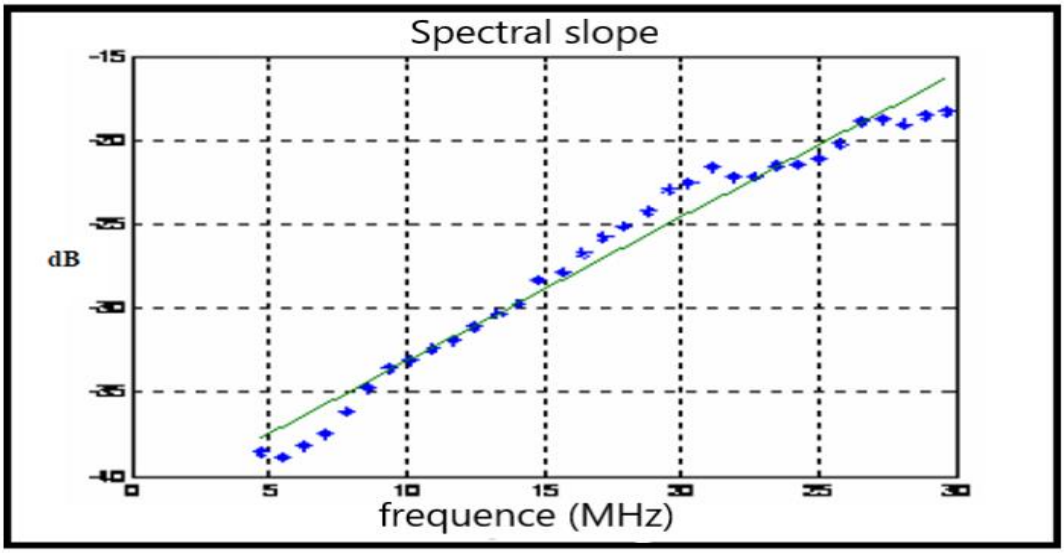


***Fig (III .4):*** *The mean backscattering coefficient curve with linear fit within the bandwidth (6-30) MHz.*

## 2.2.Method for estimating the median size of scatterers through spectral analysis:

### 2.2.1. Lizzi's Approach methode:

Our analysis deals with calibrated power spectra $S(f)$ obtained from radiofrequency (RF) signals originating from a scan set [42,48]. Following each line, the signals are weighted by a Hamming window of length L and analyzed using a Fast Fourier Transform (FFT) algorithm. The resulting power spectrum is divided by a reference spectrum (flat reflector) to compensate for diffraction and electronic system functions. The calibrated power spectra are converted to dB, and a linear least squares regression is applied to the compensated spectral attenuation ratio. Based on this, Lizzi et al. were able to determine spectral parameters such as the spectral slope (dB/MHz), the intercept, and the midband. In this study, we assume that we are dealing with a case of simple scattering where the Born approximation remains valid (meaning multiple scattering is neglected), and the tissue is located in the focal region of the transducer. We also assume that the duration of the Hamming window is much greater than the RF echo duration of each scatterer [47]. According to the method described by Lizzi et al., the calibrated spectrum, $S(f)$, is given by the relation:

$$S(f) = 4\,k^2 \iiint_{-\infty}^{\infty} R_T(\Delta x) R_D(\Delta y, \Delta z) R_G(\Delta x) e^{-j2k\Delta x} d\Delta x \qquad \textbf{(III–7)}$$

### 2.2.2. Spectral linear regression:

In the study conducted by Lizzi et al [47], it was demonstrated the possibility of approximating experimental results (calibrated spectrum) with a theoretical curve (linear regression), which allowed the determination of spectral parameters such as the slope, the intercept, and the mid-band. The expression for the spectral slope m is written as follows [47]

$$m = \frac{\int_{f_1}^{f_2} \acute{s}(f)(f-f_c)df}{\int_{f_1}^{f_2} (f-f_c)^2 df} \qquad \textbf{(III–8)}$$

$$\acute{S}(f) = 10\log S(f) = 4.34\ln E + 4.34n\ln f + 52.8\,f^2\rho^2 + 4.34\,ln\left(\rho^{2(n-1)}CQ^2\right) \qquad \textbf{(III–8)}$$

For the isotropic model, E is written as:

$$E=0.64\left[\left(\frac{2\pi}{C}\right)^4 \frac{\pi}{3}\frac{a^2}{R^2}L\right] \quad \text{n=4}$$

Finally, the spectral slope equation is written as:

$$m = 26.058.\frac{\left[b-\left(1-\frac{b^4}{4}\right)ln\left(\frac{2+b}{2-b}\right)\right]}{(b^3 f_c)} \times n - 105.5 f_c \times \rho^2 \qquad \text{(III–9)}$$

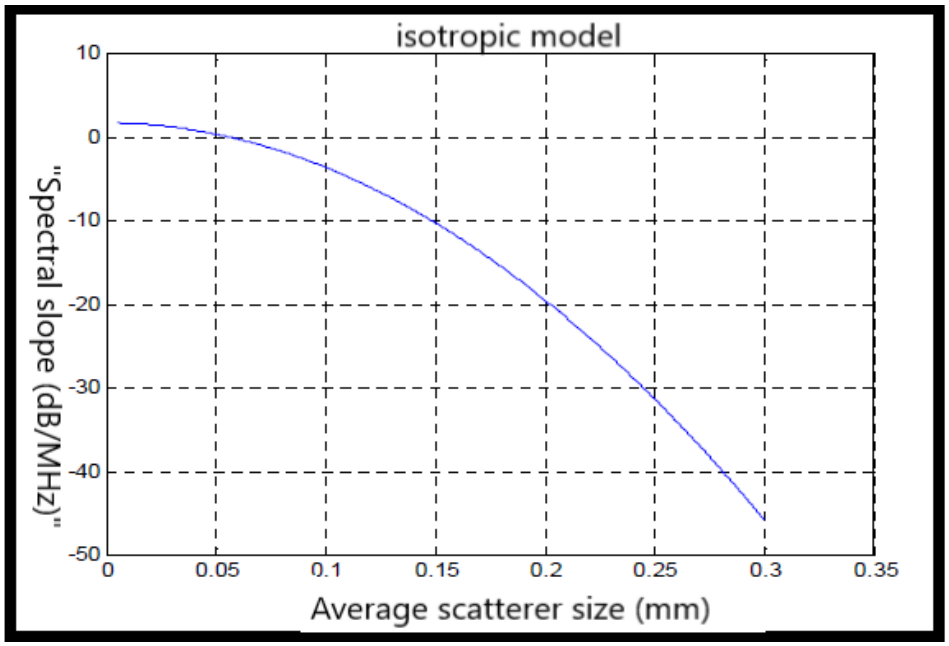


***Fig (III.6):****Spectral slope as a function of the mean scatterer size for the isotropic model within the bandwidth (6-30) MHz*

**Conclusion:**

In this chapter, we have presented the methods we used to estimate the mean size of scatterers from mean backscattering curves.

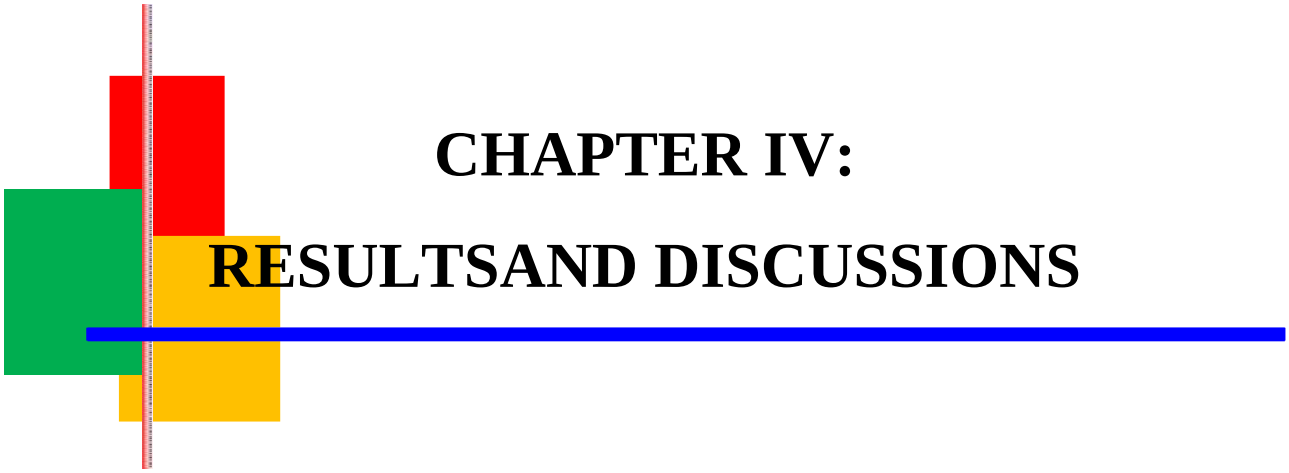

# CHAPTER IV:

# RESULTSAND DISCUSSIONS

In this chapter, we will present statistical results for tests of mean scatterer size and spectral slope by distinguishing the different stages of liver fibrosis, on liver samples.

## 1. Mean scatterer size:

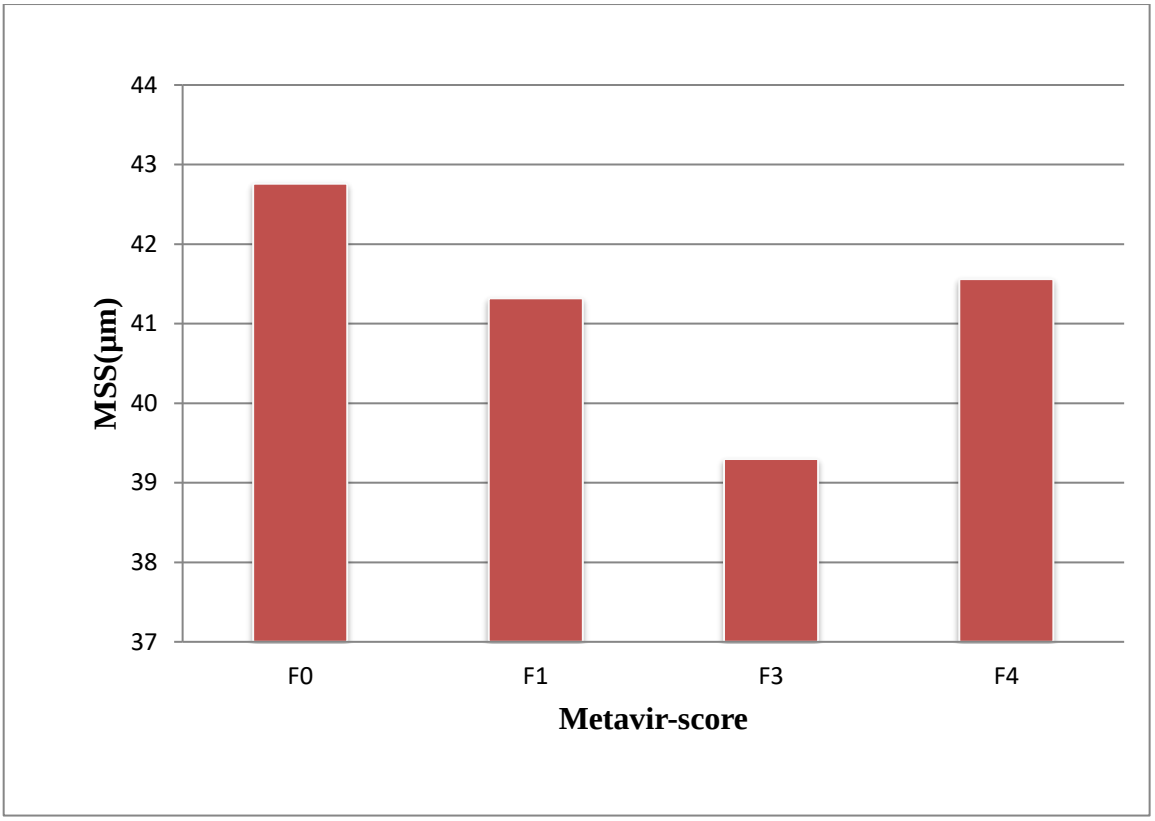


***Fig(IV.1):*** *mean scatterer size (MSS) for samples of the liver according to the Metavir-score(F0,F1,F3,F4)*

Through figure (IV.1), we notice a decrease in the value of mean scatterer size (MSS) in the different stages of fibrosis, as it is the lowest value in stage F3 due to the presence of significant liver fibrosis, then it returns to increase in F4 to equal stage F1, and this is because there is no distinction between the two stages.

**2. Spectral slope:**

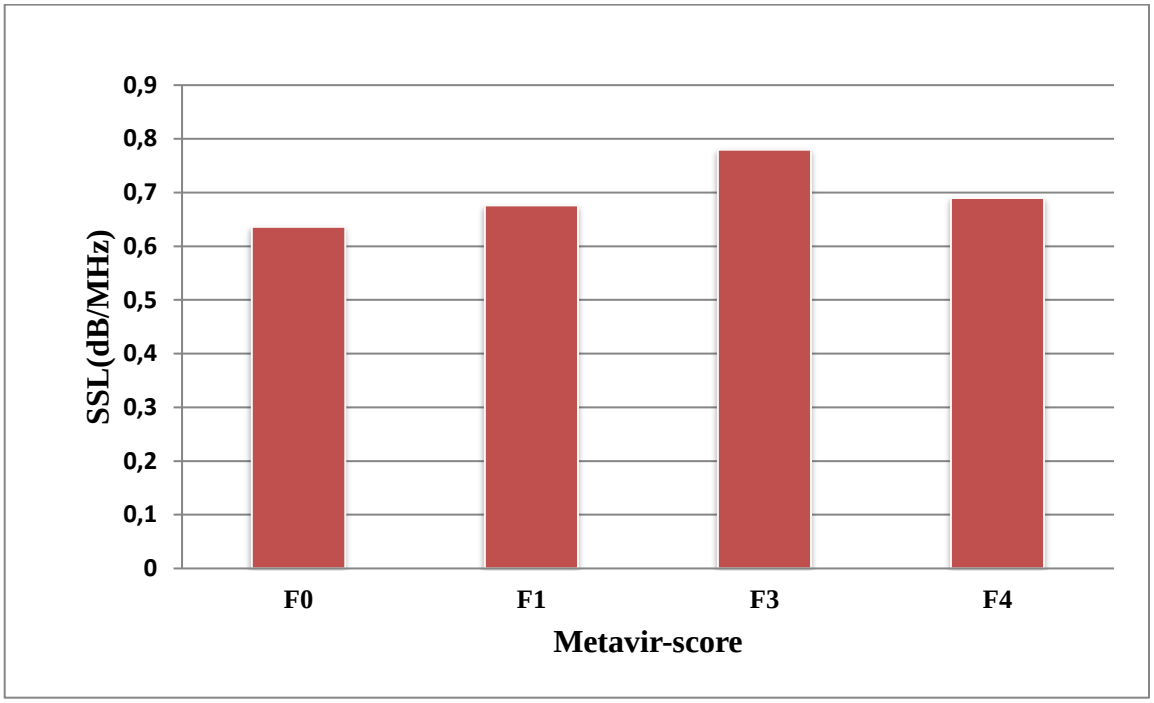


***Fig(IV.2):****Spectral slope (SSL) for samples of the liver according to the Metavir-score(F0,F1,F3,F4).*

From figure(IV.2), the spectral slope (SSL) value is lower in F0 because there is no fibrosis in the liver, and the (SSL) reaches the highest value in F3 because there is significant fibrosis in the liver, and in (F1,F4) they are equal in values because the fibrosis becomes a single mass in F4.

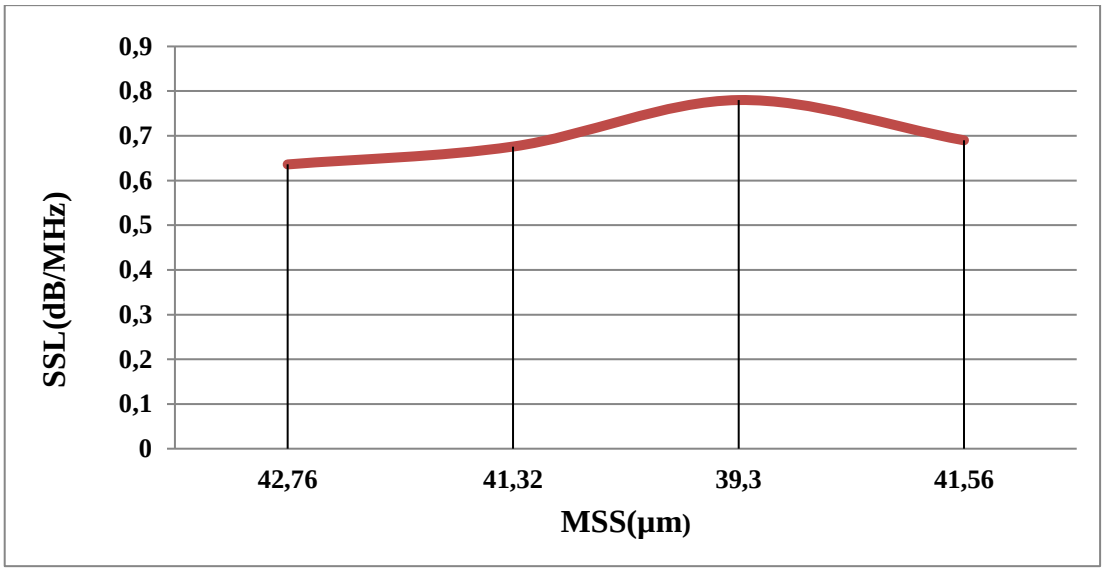


***Fig (IV.3):****The curve represents changes in spectral slope (SSL)with respect to the mean scatterer size (MSS).*

From figure (IV.3), which represents the curve of changes in the spectral slope (SSL) with respect to the mean scatterer size (MSS), we observe that when the value of (MSS) is 41.32(µm), the (SSL) value reaches 0.676(dB /MHz), and when the value of (MSS) is 39.30(µm), the (SSL) value increases to 0.78(dB /MHz). At a value of 41.56(µm), the (SSL) value decreases to 0.69(dB /MHz).

Through the results we obtained, we concluded that we could distinguish between normal and fibrotic liver, but the mean scatterer size (MSS) and spectral slope (SSL) could not distinguish between different fibrosis stages (F0, F1, F3, F4), especially between the two stages (F1, F4) as they are equal in both measured structures.

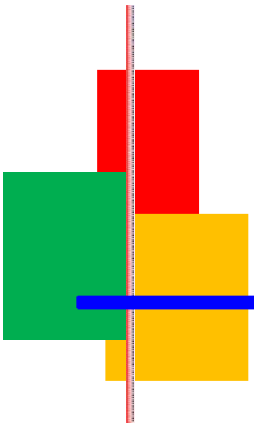

# CONCLUTION

# CONCLUTION

Based on the results of this study, we concluded that we could distinguish between normal and fibrotic liver, but mean scatter size (MSS) and spectral slope (SSL) could not distinguish between different fibrosis stages (F0, F1, F3, F4), especially between stages (F1, F4).

In our studies, fibrosis leads to tissue changes and may progress to liver cancer. For the purpose of diagnosing this disease, we tested the ability of mean scatterer size and spectral slope parameters to distinguish between normal and fibrotic liver, and to detect changes in different fibrosis stages (F0, F1, F3 and F4).

In conclusion, the research we conducted in this work aims to distinguish between different stages of liver fibrosis using different ultrasound parameters.

## References

**[1]** https://emedicine.medscape.com/article/1900159-overview?form=fpf#a3

**[2]** https://www.dreamstime.com/liver-structure-anatomical-organ-function-explanation-outline-diagram-liver-structure-anatomical-organ-function-image227450768

**[3]** From Brunicardi FC, Andersen DK, Billiar TR, et al. Schwartz's principles of surgery. 9th edition. New York: McGraw-Hill Publishing; 2010. p. 31–3; with permission. Collapse

**[4]** https://www.ncbi.nlm.nih.gov/books/NBK535438/

**[5]** https://www.medicinenet.com/fatty_liver/article.htm Medical Author: Jay W. Marks, MD Medically Reviewed on 7/18/2023

**[6]** https://www.researchgate.net/figure/Metavir-Scoring-System-for-Chronic-Hepatitis-C_tbl2_283203050

**[7]** Sun, M., &Kisseleva, T. (2015). Reversibility of liver fibrosis. Clinics and research in hepatology and gastroenterology, 39 Suppl 1(0 1), S60–S63. https://doi.org/10.1016/j.clinre.2015.06.015

**[8]** Bataller R, Brenner DA. Liverfibrosis. J Clin Invest. 2005;115:209–18. https://doi.org/10.1172/JCI24282 [PMC free article] [PubMed] [Google Scholar] [Ref list]

**[9]** Sun M, Kisseleva T. Reversibility of liver fibrosis. Clin Res Hepatol Gastroenterol. 2015;39( Suppl 1):S 60–3

**[10]** Kisseleva T, Brenner DA. Mechanisms of fibrogenesis. Exp Biol Med. 2008;233:109–22. https://doi.org/10.3181/0707-MR-190 [PubMed] [Google Scholar] [Ref list]

**[11]** https://www.aigastro.net/blog/307793-what-are-the-4-stages-of-liver-disease/

**[12]** FIG4 http://hepatoweb.com/congres/beaujon2006/hepatobeaujon2006/BEDOSSA.pdf.

**[13]** FIG 5 https://blog.radiology.virginia.edu/diagnosing-liver-fibrosis/

**[14]** Sharma B, John S. Hepatic Cirrhosis. [Updated 2022 Oct 31]. In: StatPearls [Internet]. Treasure Island (FL): StatPearls Publishing; 2024 Jan-. Available from: https://www.ncbi.nlm.nih.gov/books/NBK482419/

**[15]** Medically reviewed by Saurabh Sethi, M.D., MPH — By Jennifer Huizen — Updated on April 12, 2023 https://www.medicalnewstoday.com/articles/325073

**[16]** (NIDDK), https://www.niddk.nih.gov/

**[17]**https://i0.wp.com/post.healthline.com/wp-content/uploads/2022/01/1926368-Cirrhosis_1296x728-body.png?w=1155&h=1528

# REFERENCES

**[18]** Guidelines for the Screening, Care and Treatment of Persons with Hepatitis C Infection book 2014;

1. . Hepatitis C guidance: AASLD-IDSA recommendations for testing, managing, and treating adults infected with hepatitis C virus. Hepatology 2015;62:3.

2. . EASL-ALEH Clinical Practice Guidelines: Non-invasive tests for evaluation of liver disease severity and prognosis. J. Hepatol. 2015;63:1.

**[19]** Weerakkody Y, Bell D, Saber M, et al. METAVIR score. Reference article, Radiopaedia.org (Accessed on 15 Feb 2024) https://doi.org/10.53347/rID-51855

**[20]** https://www.researchgate.net/figure/Metavir-Scoring-System-for-Chronic-Hepatitis-C_tbl2_283203050

**[21]** Goyal N, Jain N, Rachapalli V, Cochlin DL, Robinson M. Non-invasive evaluation of liver cirrhosis using ultrasound. ClinRadiol. 2009;64:1056-66

**[22]** Talwalkar JA, Yin M, Fidler JL, Sanderson SO, Kamath PS, Ehman RL. Magnetic resonance imaging of hepatic fibrosis: emerging clinical applications. Hepatology. 2008;47:332-42

**[23]** Afdhal NH. Fibroscan (transient elastography) for the measurement of liver fibrosis. Gastroenterol Hepatol (N Y). 2012;8:605-7.

**[24]** Kim HJ, Lee HK, Cho JH, Yang HJ. Quantitative comparison of transient elastography (TE), shear wave elastography (SWE) and liver biopsy results of patients with chronic liver disease. J Phys Ther Sci. 2015;27:2465-8.[PubMed Abstract]

**[25]** Verlinden W, Bourgeois S, Gigase P, et al. Liver Fibrosis Evaluation Using Real-time Shear Wave Elastography in Hepatitis C-Monoinfected and Human Immunodeficiency Virus/Hepatitis C-Coinfected Patients. J Ultrasound Med. 2016;35:1299-308.[PubMed Abstract]

**[26]** Bohn Stafleu van Loghum, Houten (2011),Introductory Guide to Musculoskeletal Ultrasound for the Rheumatologist, the Netherlands

**[27]** https://www.news-medical.net/health/What-is-an-Ultrasound.aspx

**[28]**Liu XZ;GongXF;ZhangD;YeSG;Rui B.(2006).Ultrasonic characterization of porcine liver tissue at frequency between 25 to 55 MHz.World J Gastroenterol.12(14), 2276-2279

**[29]**Carovac,Aladin ;Smajlovic,Fahrudin;Junuzovic,dzelaludin.(2011).Application of Ultrasound in Medicine.19(3),168-171

**[30]** Bohn Stafleu van Loghum ;Houten .(2011).Introductory Guide to Musculoskeletal Ultrasound for the Rheumatologist.the Netherlands

# REFERENCES

**[31]**Carovac,Aladin;Smajlovic,Fahrudin;Junuzovic,dzelaludin.(2011).Application of Ultrasound in Medicine.19(3),168-171

**[32]**REMITA,Naamane.(2009).Caractérisation Ultrasonore de la Fibrose Hépatique par l'étude de la Taille Moyenne des Diffuseurs,1,19.

**[33]**https://aneskey.com/principles-and-physics-of-ultrasound

**[34]** John S. Mattoon ; Rance k. Sellon ;Clifford R. Berry.(2021).Small animal diagnostic ultrasound

**[35]**www.ers-education.org

**[36]**https://www.mayoclinic.org/tests-procedures/ultrasound/about/pac-2039517712

**[37]**https://www.nysora.com/physics-of-ultrasound/

**[38]**https://www.researchgate.net/figure/Scattering-When-the-ultrasound-wave-encounters-an-irregular-interface-it-scatters-in_fig4_276338051

**[39]**https://info.isradiology.org/docs_books/basic/Chapter3.pdf

**[40]**M. PILLAI، P.BRIGGS، J.M. BRIDSON.(2018).ULTRASOUND in Reproductive Healthcare Practice.CAMBRIDGE UNIVERSITY PRESS.

**[41]** https://fr.slideshare.net/abhijitcool18/application-of-ultrasound-in-separation-process

**[42]** F.L. Lizzi, M. Greendaum, E.J. Feleppa, and Marek Elbaum, "Theoretical framework for spectrum analysis in ultrasonic tissue characterization", J. Acoust. Soc. Am., 73:1366-1373, 1983.

**[43]** F. M. Inssana and D. G. Brown., "Acoustic scattering theory applied to soft biological tissues", in Ultrasonic Scattering in Biological Tissues., Boca Raton, FL: CRC press. p. 75-124, 1993

**[44]** V. Roberjot., S. Bridal. Lori., P. Laugier., and G. Berger., «Absolute backscatter coefficient over a wide range of frequency in a tissue-mimicking phantom containing two populations of scatterers», IEEE Trans. Sonic and Ultr., vol 43, no. 5, September, 1996

**[45]** K. A. Wear, B. A. Garra, and T. J. Hall., Measurements of ultrasonic backscatter coefficient in human liver and kidney in vivo. J. Acoust. Soc. Am :p. 1852-1857, 1995

**[46]** M. Fink, J. F. Cardoso, and P. Laugier., Analyse des effets de la diffraction en échographie médicale. Ultrason. Imaging, vol. 26(1-2): pp. 59-80, 1984.

**[47]** F.L. Lizzi, M. Astro, A. Kalisz, T. Liu, D. J. Coleman, R. Silverman, R. Ursea, M. Rondeau, "Ultrasonic spectrum analysis for assays of different scatterer morphologies: Theory and very-high frequency clinical results," IEEE Ultrasonics symposium. 0-7803-3615-1/96/5.00, 1996.

**[48]** E.J. Feleppa and F.L. Lizzi, “Ophthalmological tissue characterization by scattering in Ultrasonic Scattering in Biological Tissues”, K. Shung and G. Theime, eds, Boca Raton, CRC Press, pp.393-408, 1993